DYNAMIC CRACK PROPAGATION IN PIEZOELECTRIC MATERIALS SUBJECTED TO DYNAMIC BODY FORCES FOR VACUUM BOUNDARY

X.-H. Chen * **C.-C. Ma** **

Department of Mechanical Engineering
National Taiwan University
Taipei, Taiwan 10617, R.O.C.

Y.-S. Ing ***

Department of Aerospace Engineering
Tamkang University
Tamsui, Taiwan 25137, R.O.C.

ABSTRACT

The problem of a semi-infinite propagating crack in the piezoelectric material subjected to a dynamic anti-plane concentrated body force is investigated in the present study. It is assumed that between the growing crack surfaces there is a permeable vacuum free space, in which the electrostatic potential is nonzero. It is noted that this problem has characteristic lengths and a direct attempt towards solving this problem by transform and Wiener-Hopf techniques [1] is not applicable. This paper proposes a new fundamental solution for propagating crack in the piezoelectric material and the transient response of the propagating crack is determined by superposition of the fundamental solution in the Laplace transform domain. The fundamental solution represents the responses of applying exponentially distributed loadings in the Laplace transform domain on the propagating crack surface. Exact analytical transient solutions for the dynamic stress intensity factor and the dynamic electric displacement intensity factor are obtained by using the Cagniard-de Hoop method [2,3] of Laplace inversion and are expressed in explicit forms. Finally, numerical results based on analytical solutions are calculated and are discussed in detail.

Keywords : Crack propagation, Piezoelectric material, Superposition, Dynamic stress intensity factor, Dynamic electric displacement intensity factor.

1. INTRODUCTION

More than a century has passed since the Curie brothers discovered the piezoelectric effect in 1880. Today, over a hundred piezoelectric materials or composites are used in many engineering applications [4]. Due to their intrinsic electromechanical coupling behaviors, piezoelectric materials, particularly piezoelectric ceramics, have been widely used for applications such as sensors, filters, ultrasonic generators and actuators. Because of the brittle properties for most piezoelectric materials, the failure analysis of piezoelectric devices is needed. It was found in many applications that flaws contained in piezoelectric materials may lead to serious danger. Therefore, it is necessary to study the dynamic fracture mechanic of piezoelectric materials. Since the inherent time dependence of a dynamic fracture process results in mathematical models that are more complicate than equivalent quasi-static models, hence most of the analyses done in the literature are quasi-static.

About forty years ago, Bleustein [5] and Gulyaev [6] simultaneously discovered that there exists a shear horizontal (SH) electro-acoustic surface mode in a class of transversely isotropic piezoelectric media, which is known today as the BG surface wave. The BG surface wave is a unique result in the repertoire of SAW theory, because it has no counterpart in purely elastic solids and the BG surface wave has become one of the cornerstones for the modern electro-acoustic technology. As in the case of the Stoneley wave [7], whose mechanical displacements are in the sagittal plane, the amplitude of this wave decreases with distance away from the interface into both media. One of the most important and basic issues of studying fracture mechanics of piezoelectric materials is the electrode or vacuum boundary condition on the crack surface. The theory of electro-acoustic wave scattering in piezoelectric materials is still an open subject. This is because the fully coupled Christoffel-Maxwell equations of piezoelectric media are analytically intractable and the simplified wave equations under the quasi-static approximation are not mathematically well-posed. In an attempt to regularize wave equations for piezoelectric media while still retaining the simplicity of the quasi-static approximation, a few regularization procedures have been proposed [8]. These developments provide a foundation on which to establish a much needed electro-acoustic wave scattering theory for piezoelectric materials.

In the study of crack propagation, Yoffe [9] was the first one to investigate a steady-state crack growth problem of a crack of fixed length propagating in an infinite and purely elastic body subjected to a uniform remote tensile stress. Subsequently, many researchers

* Ph.D. candidate ** Professor, corresponding author *** Professor

were devoted to the study of crack propagation for purely elastic solids. For example, it was shown by Achenbach [10] that a horizontally polarized shear wave can incite transient extension of a crack. The dynamic fracture problem of a semi-infinite crack extending non-uniformly in an isotropic elastic solid subjected to stress wave loading was considered by Freund [11]. It was found that the mode I and mode II stress intensity factors each have the form of the product of a universal function of instantaneous crack tip speed with the stress intensity factor for an equivalent stationary crack. Ma and Hou [12,13] analyzed a series of problems of an unbounded medium containing a semi-infinite crack subjected to impact loadings. For piezoelectric crack problem, Li and Mataga [14,15] first obtained transient closed-form solutions for dynamic stress and electric displacement intensities and dynamic energy release rate of a propagating crack in homogeneous hexagonal piezoelectric materials. They assumed that the crack surfaces are electrode- or vacuum-type boundary conditions and the dynamic anti-plane point loading was initially applied at the stationary crack tip. Hence there is no characteristic length presented in their problems. Ing and Ma [16,17] solved the problem of a finite crack subjected to a dynamic anti-plane point loading and a horizontally polarized shear wave in isotropic solids, but only dynamic stress intensity factors were obtained in closed forms. Chen and Yu [18] studied the problem of anti-plane Yoffe's crack in an unbounded piezoelectric medium. Kwon and Lee [19] investigated the crack problem of an infinitely long piezoelectric ceramic strip containing a Griffith crack moving with constant velocity. The problem of electro-acoustic wave scattering by an interfacial stationary crack between two dissimilar piezoelectric half-spaces subjected to both incident plane SH acoustic waves and incident plane electrical waves was analyzed by To *et al.* [20]. The problem of an unbounded elastic solid containing a semi-infinite crack subjected to a pair of concentrated point loadings on the crack faces has been studied by Freund [21]. The transient problem of a stationary crack for purely piezoelectric solids was studied by Ing and Wang [22]. A powerful and efficient methodology based on superimposing a fundamental solution in the Laplace transform domain was proposed by Tsai and Ma [23]. Exact transient closed-form solutions of stress and dynamic stress-intensity factors for a stationary semi-infinite crack subjected to a suddenly applied dynamic body force in an unbounded medium have been obtained for the in-plane case. This fundamental solution and superposition methodology have also been successfully applied by Ma and Chen [24] to solve the more complicated problem of a half-plane containing a stationary semi-infinite inclined crack for anti-plane deformation. This superposition methodology was generalized and applied to analyze the propagating crack interacting with boundaries for in-plane deformation by Tsai and Ma [25,26], but only the effects of first few reflected waves from the boundaries were taken into account. Yang *el al.* [27] proposed fracture criteria for the piezoelectric materials.

In this paper, the transient response of a semi-infinite propagating crack subjected to dynamic anti-plane concentrated loading in the piezoelectric material is investigated. A new fundamental solution is derived and the transient solution is determined by superposition of the fundamental solution in the Laplace transform domain. The proposed fundamental solution is an exponentially distributed traction applied on the propagating crack faces. Exact analytical transient solutions for the dynamic stress intensity factor and the dynamic electric displacement intensity factor are obtained. Numerical results are presented based on the analytical solutions and are discussed in detail.

2. THE FUNDAMENTAL PROBLEM AND FUNDAMENTAL SOLUTIONS

In this section, a fundamental problem is proposed and the associated fundamental solutions will be presented which will be used to solve the crack propagation problem with characteristic lengths in the next section. Consider a piezoelectric material containing a semi-infinite crack that lies on the negative ξ-axis and propagates with a constant velocity v along the crack tip line. It is assumed that between the growing crack surfaces there is a permeable vacuum free space, in which the electrostatic potential is nonzero. The geometrical configuration is shown in Fig. 1.

If we consider only the out-of-plane displacement and the in-plane electric fields, the governing equations for a hexagonal piezoelectric material (6mm) can be described in the fixed coordinate system $x-y$ by

$$c_{44}\nabla^2 w + e_{15}\nabla^2\phi = \rho\ddot{w}\,, \tag{1}$$

$$e_{15}\nabla^2 w - \varepsilon_{11}\nabla^2\phi = 0\,, \tag{2}$$

where $w = w(x, y, t)$ is the anti-plane displacement in the z-direction (which is assumed to aligned with the hexagonal symmetry axis), $\phi = \phi\,(x, y, t)$ is the electric potential, c_{44} is the elastic modulus measured in a constant electric field, ε_{11} is the dielectric permittivity measured at a constant strain, e_{15} is the piezoelectric constant and ρ is the material density. $\nabla^2 = \partial^2/\partial x^2 + \partial^2/\partial y^2$ is the in-plane Laplacian and a dot denotes material time derivative. The constitutive equations for the piezoelectric material can be expressed as

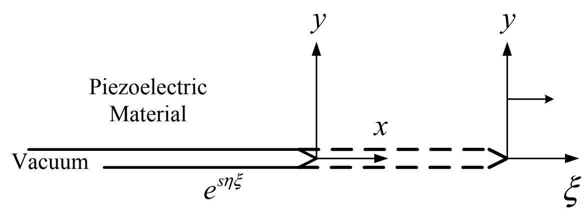

Fig. 1 Configuration and coordinate systems of a propagating crack in the piezoelectric material

$$\tau_{yz} = c_{44}\frac{\partial w}{\partial y} + e_{15}\frac{\partial \phi}{\partial y}, \tag{3}$$

$$\tau_{xz} = c_{44}\frac{\partial w}{\partial x} + e_{15}\frac{\partial \phi}{\partial x}, \tag{4}$$

$$D_y = e_{15}\frac{\partial w}{\partial y} - \varepsilon_{11}\frac{\partial \phi}{\partial y}, \tag{5}$$

$$D_x = e_{15}\frac{\partial w}{\partial x} - \varepsilon_{11}\frac{\partial \phi}{\partial x}, \tag{6}$$

where τ_{yz} and τ_{xz} are the shear stress components and D_y and D_x are the electric displacements.

In analyzing the problem of a crack propagating with a constant velocity, it is convenient to express the relevant equations in the moving ξ-y coordinates. The coordinate ξ defined by $\xi = x - vt$ is fixed with respect to the moving crack tip. Making use of the transformation, the governing and constitutive equations for a hexagonal piezoelectric material and the Maxwell equation in the vacuum strip can be rewritten as follows

$$(1 - b^2v^2)\frac{\partial^2 w}{\partial \xi^2} + \frac{\partial^2 w}{\partial y^2} + 2b^2 v\frac{\partial^2 w}{\partial \xi \partial t} - b^2\frac{\partial^2 w}{\partial t^2} = 0, \tag{7}$$

$$\frac{\partial^2 \psi}{\partial \xi^2} + \frac{\partial^2 \psi}{\partial y^2} = 0, \tag{8}$$

$$\frac{\partial^2 \phi^v}{\partial \xi^2} + \frac{\partial^2 \phi^v}{\partial y^2} = 0, \tag{9}$$

$$\tau_{yz} = \bar{c}_{44}\frac{\partial w}{\partial y} + e_{15}\frac{\partial \psi}{\partial y}, \tag{10}$$

$$\tau_{\xi z} = \bar{c}_{44}\frac{\partial w}{\partial \xi} + e_{15}\frac{\partial \psi}{\partial \xi}, \tag{11}$$

$$D_y = -\varepsilon_{11}\frac{\partial \psi}{\partial y}, \tag{12}$$

$$D_\xi = -\varepsilon_{11}\frac{\partial \psi}{\partial \xi}, \tag{13}$$

where

$$\psi = \phi - \frac{e_{15}}{\varepsilon_{11}} w \tag{14}$$

and

$$\bar{c}_{44} = c_{44} + \frac{e_{15}^2}{\varepsilon_{11}} \tag{15}$$

is the piezoelectrically stiffened elastic constant. ϕ^v is the electric potential in the vacuum strip. The solution for an exponentially distributed loading applied at the crack faces in the transform domain will be referred to as the fundamental solutions. For such a situation, the mixed boundary conditions in the Laplace transform domain can be described as follows

$$\bar{\tau}_{yz}(\xi, 0, s) = e^{s\eta\xi} \text{ for } -\infty < \xi < 0, \tag{16}$$

$$\bar{w}(\xi, 0, s) = 0 \text{ for } 0 < \xi < \infty, \tag{17}$$

$$\bar{D}_y(\xi, 0^+, s) = \bar{D}_y^v(\xi, 0^+, s) \text{ for } -\infty < \xi < 0, \tag{18}$$

$$\bar{\phi}(\xi, 0^+, s) = \bar{\phi}^v(\xi, 0^+, s) \text{ for } -\infty < \xi < 0, \tag{19}$$

where s is the Laplace transform parameter and η is a constant. D_y^v is the electric displacement in the vacuum strip. The coordinate ξ is fixed with respect to the moving crack tip. The over-bar symbol is used for denoting the transform on time t. The one-sided Laplace transform over time t and the bilateral Laplace transform on the spatial variable ξ are defined by

$$\bar{w}(\xi, y, s) = \int_0^\infty w(\xi, y, t)\, e^{-st} dt, \tag{20}$$

$$\bar{w}^*(\lambda, y, s) = \int_{-\infty}^{\infty} \bar{w}(\xi, y, s)\, e^{-s\lambda\xi} d\xi, \tag{21}$$

where s which is the Laplace transform parameter is a positive real number, large enough to ensure the convergence of the integral and λ is a complex variable.

The general solutions for $\bar{w}^*$, $\bar{\psi}^*$ and $\bar{\phi}^{v^*}$ in the double transformed domain can be obtained as follows

$$\bar{w}^*(\lambda, y, s) = A(\lambda, s)\, e^{-s\alpha^*(\lambda)y}, \tag{22}$$

$$\bar{\psi}^*(\lambda, y, s) = B(\lambda, s) e^{-s\beta^*(\lambda)y}, \tag{23}$$

$$\bar{\phi}^{v^*}(\lambda, y, s) = C(\lambda, s) e^{s\beta^*(\lambda)y}, \tag{24}$$

where

$$\begin{aligned}\alpha^*(\lambda) &= \sqrt{b^2 - \lambda^2 + b^2v^2\lambda^2 - 2b^2v\lambda} \\ &= \sqrt{b + \lambda(1 - bv)}\sqrt{b - \lambda(1 + bv)} = \alpha_+^*(\lambda)\alpha_-^*(\lambda),\end{aligned} \tag{25}$$

$$\begin{aligned}\beta^*(\lambda) &= \lim_{\varepsilon \to 0}\sqrt{\varepsilon^2 - \lambda^2} = \lim_{\varepsilon \to 0}\sqrt{\varepsilon + \lambda}\sqrt{\varepsilon - \lambda} \\ &= \lim_{\varepsilon \to 0}\beta_+^*(\lambda)\beta_-^*(\lambda),\end{aligned} \tag{26}$$

and

$$b = 1/c = \sqrt{\rho/\bar{c}_{44}} \tag{27}$$

is the slowness of the shear wave in the piezoelectric material and c is the velocity of the shear wave in the piezoelectric material. Note that, $\varepsilon \to 0^+$ is an auxiliary positive real perturbation parameter. Application of the multiple Laplace transforms to (16) and (17) yields

$$\overline{\tau}_{yz}^*(\lambda, 0, s) = \frac{1}{s(\eta - \lambda)} + \overline{\tau}_+^*(\lambda, s) \text{ for } -\infty < \xi < \infty, \tag{28}$$

$$\overline{w}^*(\lambda, 0, s) = \overline{w}_-^*(\lambda, s) = A(\lambda, s) \text{ for } 0 < \xi < \infty, \tag{29}$$

where $\mathrm{Re}(\eta) > \mathrm{Re}(\lambda)$. The unknown function τ_+ is defined to be the shear stress τ_{yz} on the plane $y = 0$ for $0 < \xi < \infty$. Likewise, $\overline{w}_-^*$ is defined to be the displacement in the z-direction on the plane $y = 0$ for $0 < \xi < \infty$. Substitution of (22) ~ (24) into (28) ~ (29) leads to

$$-\overline{c}_{44}A(\lambda, s)[\alpha^*(\lambda) - k_v^2\beta^*(\lambda)] = \frac{1}{s^2(\eta - \lambda)} + \frac{1}{s}\overline{\tau}_+^*(\lambda, s), \tag{30}$$

where $k_v^2 = (e_{15}^2/\overline{c}_{44}\varepsilon_{11})[\varepsilon_0/(\varepsilon_0 + \varepsilon_{11})]$ is the electromechanical coupling coefficient for the vacuum boundary condition and ε_0 is the dielectric permittivity in the vacuum strip. Then rewriting (30) and the Wiener-Hopf equation is derived as

$$-\overline{c}_{44}\overline{w}_-^*(\lambda, s)[\alpha^*(\lambda) - k_v^2\beta^*(\lambda)] = \frac{1}{s^2(\eta - \lambda)} + \frac{1}{s}\overline{\tau}_+^*(\lambda, s). \tag{31}$$

It is noted that the bracketed term $\alpha^*(\lambda) - k_v^2\beta^*(\lambda)$ in the left-hand side of (31) corresponds to the second kind of Bleustein-Gulyaev wave function (Bleustein [5]; Gulyaev [6]). The Bleustein-Gulyaev wave function will be decomposed and we introduce a new function $S^*(\lambda)$ by defining

$$S^*(\lambda) = \frac{\alpha^*(\lambda) - k_v^2\beta^*(\lambda)}{\sqrt{1 + (c_{bg} - v)\lambda}\sqrt{1 - (c_{bg} + v)\lambda}} \cdot \frac{\sqrt{c_{bg}^2 - v^2}}{\sqrt{1 - b^2v^2} - k_v^2}, \tag{32}$$

where

$$c_{bg} = \frac{\sqrt{1 - k_v^4}}{b} \tag{33}$$

is the Bleustein-Gulyaev wave speed in classical piezoelectric theory with vacuum boundary condition. It is assumed in this study that the crack speed v does not exceed c_{bg}. Under this assumption, the function $S^*(\lambda)$ has the properties that $S^*(\lambda) \to 1$ as $|\lambda| \to \infty$, and $S^*(\lambda)$ has neither poles nor zeros in the λ-plane by cuts along $-1/(c_{bg} - v) < \lambda < -\varepsilon$ and $\varepsilon < \lambda < 1/(c_{bg} + v)$. By using the general product factorization method, $S^*(\lambda)$ can be further decomposed as the product of two regular functions $S_+^*(\lambda)$ and $S_-^*(\lambda)$, where

$$S_+^*(\lambda) = \sqrt{\frac{1/(c_{bg} - v) + \lambda}{1/(c - v) + \lambda}}Q_+^*(\lambda) \tag{34}$$

and

$$S_-^*(\lambda) = \sqrt{\frac{1/(c_{bg} + v) - \lambda}{1/(c + v) - \lambda}}Q_-^*(\lambda), \tag{35}$$

in which

$$Q_+^*(\lambda) = \exp\left\{\frac{1}{\pi}\int_\varepsilon^{\frac{1}{c-v}} \tan^{-1}\left[\frac{k_v^2\sqrt{z^2 - \varepsilon^2}}{\alpha^*(-z)}\right]\frac{dz}{z + \lambda}\right\}, \tag{36}$$

$$Q_-^*(\lambda) = \exp\left\{\frac{1}{\pi}\int_\varepsilon^{\frac{1}{c+v}} \tan^{-1}\left[\frac{k_v^2\sqrt{z^2 - \varepsilon^2}}{\alpha^*(z)}\right]\frac{dz}{z - \lambda}\right\}. \tag{37}$$

The bracketed term $\alpha^*(\lambda) - k_v^2\beta^*(\lambda)$ in the left- hand side of (31) can be decomposed by introducing a new function $S^*(\lambda)$ which can be further decomposed as the product of two regular functions $S_+^*(\lambda)$ and $S_-^*(\lambda)$. Then, (31) is expressed as

$$-\overline{c}_{44}(\sqrt{1 - b^2v^2} - k_v^2)\frac{1/(c_{bg} + v) - \lambda}{\sqrt{1/(c + v) - \lambda}}Q_-^*(\lambda)\overline{w}_-^*(\lambda, s) = \frac{M_+^*(\lambda)}{s^2(\eta - \lambda)} + \frac{M_+^*(\lambda)}{s}\overline{\tau}_+^*(\lambda, s), \tag{38}$$

where

$$M_+^*(\lambda) = \frac{\sqrt{1/(c - v) + \lambda}}{[1/(c_{bg} - v) + \lambda]\,Q_+^*(\lambda)}. \tag{39}$$

The first term on the right-hand side of (38) is regular for $\mathrm{Re}(\lambda) > -\varepsilon$, except for the pole at $\lambda = \eta$. The pole can be removed and (38) can be rearranged into the desired form

$$-\overline{c}_{44}(\sqrt{1 - b^2v^2} - k_v^2)\frac{1/(c_{bg} + v) - \lambda}{\sqrt{1/(c + v) - \lambda}}Q_-^*(\lambda)\overline{w}_-^*(\lambda, s) - \frac{M_+^*(\eta)}{s^2(\eta - \lambda)} = \frac{M_+^*(\lambda) - M_+^*(\eta)}{s^2(\eta - \lambda)} + \frac{M_+^*(\lambda)}{s}\overline{\tau}_+^*(\lambda, s). \tag{40}$$

The left-hand side of this equation is regular for $\mathrm{Re}(\lambda) < \varepsilon$, while the right-hand side is regular for $\mathrm{Re}(\lambda) > -\varepsilon$. Applying the analytic continuation argument, therefore, each side of (40) represents a single entire function, say $E^*(\lambda)$. From Liouville's theorem, the bounded entire function $E^*(\lambda)$ is a constant. The magnitude of the constant can be obtained from order conditions on $E^*(\lambda)$ as $|\lambda| \to \infty$, which in turn are obtained from order conditions on the dependent field variables in the vicinity of $\xi = 0$. Consequently, $\overline{\tau}_+(\xi, 0, s)$ is expected to be square root singular near $\xi = 0$, *i.e.* $\overline{\tau}_+(\xi, 0, s) = O(|\xi|^{-1/2})$ as $\xi \to 0^+$. By using of the Abelian theorem, $E^*(\lambda)$ vanishes identically, and we can solve for

$\overline{\tau}_{+}^{*}(\lambda, s)$ and $\overline{w}_{-}^{*}(\lambda, s)$ as follows

$$\overline{\tau}_{+}^{*}(\lambda, s)=\frac{1}{s(\eta-\lambda)}\left[\frac{M_{+}^{*}(\eta)}{M_{+}^{*}(\lambda)}-1\right], \tag{41}$$

$$\overline{w}_{-}^{*}(\lambda, s)=\frac{-M_{+}^{*}(\eta)\sqrt{1/(c+v)-\lambda}}{\overline{c}_{44}(\sqrt{1-b^2v^2}-k_v^2)s^2(\eta-\lambda)[1/(c_{bg}+v)-\lambda]\,Q_{-}^{*}(\lambda)}. \tag{42}$$

Substituting (41) and (42) into (22) ~ (24), and then inverting the two-sided Laplace transform, fundamental solutions for the proposed fundamental problem in the Laplace transform domain are obtained as follows

$$\overline{w}(\xi, y, s)=\frac{-1}{2\pi i}\int_{\Gamma_\lambda}\frac{M_{+}^{*}(\eta)\sqrt{1/(c+v)-\lambda}\,e^{s[-\alpha^*(\lambda)y+\lambda\xi]}}{\overline{c}_{44}(\sqrt{1-b^2v^2}-k_v^2)\,s(\eta-\lambda)[1/(c_{bg}+v)-\lambda]\,Q_{-}^{*}(\lambda)}d\lambda, \tag{43}$$

$$\begin{aligned}\overline{\tau}_{\xi z}(\xi, y, s)=&\frac{-1}{2\pi i}\int_{\Gamma_\lambda}\frac{M_{+}^{*}(\eta)\lambda\sqrt{1/(c+v)-\lambda}\,e^{s[-\alpha^*(\lambda)y+\lambda\xi]}}{(\sqrt{1-b^2v^2}-k_v^2)(\eta-\lambda)[1/(c_{bg}+v)-\lambda]\,Q_{-}^{*}(\lambda)}d\lambda\\&+\frac{1}{2\pi i}\int_{\Gamma_\lambda}\frac{k_v^2M_{+}^{*}(\eta)\lambda\sqrt{1/(c+v)-\lambda}\,e^{s[-\beta^*(\lambda)y+\lambda\xi]}}{(\sqrt{1-b^2v^2}-k_v^2)(\eta-\lambda)[1/(c_{bg}+v)-\lambda]\,Q_{-}^{*}(\lambda)}d\lambda,\end{aligned} \tag{44}$$

$$\begin{aligned}\overline{\tau}_{yz}(\xi, y, s)=&\frac{1}{2\pi i}\int_{\Gamma_\lambda}\frac{M_{+}^{*}(\eta)\,\alpha^*(\lambda)\sqrt{1/(c+v)-\lambda}\,e^{s[-\alpha^*(\lambda)y+\lambda\xi]}}{(\sqrt{1-b^2v^2}-k_v^2)(\eta-\lambda)[1/(c_{bg}+v)-\lambda]\,Q_{-}^{*}(\lambda)}d\lambda\\&-\frac{1}{2\pi i}\int_{\Gamma_\lambda}\frac{k_v^2M_{+}^{*}(\eta)\,\beta^*(\lambda)\sqrt{1/(c+v)-\lambda}\,e^{s[-\beta^*(\lambda)y+\lambda\xi]}}{(\sqrt{1-b^2v^2}-k_v^2)(\eta-\lambda)[1/(c_{bg}+v)-\lambda]\,Q_{-}^{*}(\lambda)}d\lambda,\end{aligned} \tag{45}$$

$$\overline{D}_{\xi}(\xi, y, s)=\frac{-1}{2\pi i}\int_{\Gamma_\lambda}\frac{k_v^2\varepsilon_{11}M_{+}^{*}(\eta)\lambda\sqrt{1/(c+v)-\lambda}\,e^{s[-\beta^*(\lambda)y+\lambda\xi]}}{e_{15}(\sqrt{1-b^2v^2}-k_v^2)(\eta-\lambda)[1/(c_{bg}+v)-\lambda]\,Q_{-}^{*}(\lambda)}d\lambda, \tag{46}$$

$$\overline{D}_{y}(\xi, y, s)=\frac{1}{2\pi i}\int_{\Gamma_\lambda}\frac{\varepsilon_{11}k_v^2M_{+}^{*}(\eta)\,\beta^*(\lambda)\sqrt{1/(c+v)-\lambda}\,e^{s[-\beta^*(\lambda)y+\lambda\xi]}}{e_{15}(\sqrt{1-b^2v^2}-k_v^2)(\eta-\lambda)[1/(c_{bg}+v)-\lambda]\,Q_{-}^{*}(\lambda)}d\lambda. \tag{47}$$

The corresponding results of the dynamic stress intensity factor and the dynamic electric displacement intensity factor expressed in the Laplace transform domain are

$$\overline{K}_{III}^{(\tau)}(s)=\lim_{\xi\to 0}\sqrt{2\pi\xi}\,\overline{\tau}_{yz}(\xi, 0, s)=-\sqrt{\frac{2}{s}}M_{+}^{*}(\eta) \tag{48}$$

and

$$\overline{K}_{III}^{(D)}(s)=\lim_{\xi\to 0}\sqrt{2\pi\xi}\,\overline{D}_{y}(\xi, 0, s)=-\sqrt{\frac{2}{s}}\frac{\varepsilon_{11}k_v^2M_{+}^{*}(\eta)}{e_{15}(\sqrt{1-b^2v^2}-k_v^2)}, \tag{49}$$

respectively.

3. TRANSIENT SOLUTIONS OF DYNAMIC INTENSITY FACTORS

As shown in Fig. 2, a semi-infinite crack lying in the piezoelectric material is initially stress free and at rest. At time $t = 0$, a dynamic anti-plane concentrated loading with magnitude $2p$ is applied at $x = l$, $y = h$. The time dependence of the concentrated loading is represented by the Heaviside function $\mathrm{H}(t)$. After a delay time br ($r=\sqrt{l^2+h^2}$), the stress wave arrives at the crack tip and the crack begins to extend at a constant velocity ν. The moving coordinate system (ξ, y) is attached to the moving crack tip. The relation between x and ξ is $x = \xi + v(t - br)$. It is assumed that between the growing crack surfaces, there is a permeable vacuum free space, in which the electrostatic potential is nonzero. The jump condition for the applied loading is represented by

$$\tau_{yz}(x, h^+, t)-\tau_{yz}(x, h^-, t)=-2p\delta(x-l)\,\mathrm{H}(t). \tag{50}$$

The incident field generated by the concentrated loading can be expressed in the Laplace transform domain as follows

$$\overline{\tau}_{yz}(\xi, 0, s)=\frac{1}{2\pi i}\int_{\Gamma_\lambda}\left(\frac{-pd}{d-\lambda}e^{-s[\alpha^*(\lambda)h+\lambda l]-s\lambda(vbr)}\right)e^{s\lambda\xi}d\lambda, \tag{51}$$

where $d = 1/v$. The applied traction on the crack faces as indicated in (51) has the functional form $e^{s\lambda\xi}$. Since the solutions of applying traction $e^{s\xi\eta}$ on crack faces have been solved in the previous section, the reflected and diffracted fields generated from the crack can be constructed by superimposing the incident wave traction that is equal to (51). Since the dynamic stress intensity factor and electric displacement intensity factor are the key parameters in characterizing dynamic crack growth, we will focus our attention mainly on the determination of transient behavior for these quantities. The dynamic stress intensity factor expressed in the Laplace transform domain can be obtained from (48) and (51) as follows

$$\overline{K}_{III}^{(\tau)}(s)=\frac{1}{2\pi i}\int_{\Gamma_\eta}\frac{-pd}{d-\eta}e^{-s[\alpha^*(\eta)h+\eta l]}e^{s\eta(-vbr)}\left\{\frac{-\sqrt{2}M_{+}^{*}(\eta)}{\sqrt{s}}\right\}d\eta. \tag{52}$$

From (49) and (51), the dynamic electric displacement intensity factor is

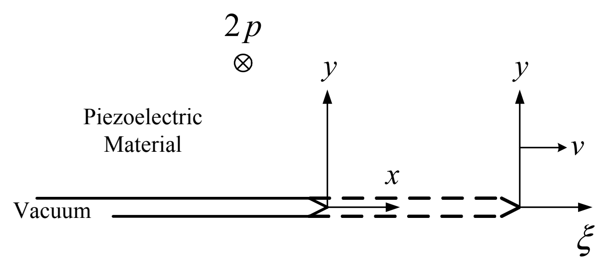

Fig. 2 Configuration and coordinate systems of a propagating crack subjected to a dynamic anti-plane body force in the piezoelectric material

$$\bar{K}_{III}^{(D)}(s) = \frac{1}{2\pi i}\int_{\Gamma_\eta} \frac{-pd}{d-\eta} e^{-s[\alpha^*(\eta)h+\eta l]} e^{s\eta(-vbr)} \left\{ \frac{-\varepsilon_{11}k_v^2\sqrt{2}M_+^*(\eta)}{e_{15}(\sqrt{1-b^2v^2}-k_v^2)\sqrt{s}} \right\} d\eta \,. \quad (53)$$

By using the Cagniard method of Laplace inversion, the relevant dynamic intensity factors in time domain can be obtained as follows

$$K_{III}^{(\tau)}(t) = \sqrt{\frac{2}{\pi^3}}pd\int_0^t \mathrm{Im}\left\{\left[\frac{M_+^*(\eta^+)}{d-\eta^+}\frac{\partial\eta^+}{\partial t}\right]_{t=\tau}\frac{1}{\sqrt{t-\tau}}\right\}d\tau\,\mathrm{H}(t-br)$$
$$+\sqrt{\frac{2}{\pi^3}}pd\int_0^t \mathrm{Im}\left\{\left[\frac{M_+^*(\eta_i^+)}{d-\eta_i^+}\frac{\partial\eta_i^+}{\partial t}\right]_{t=\tau}\frac{1}{\sqrt{t-\tau}}\right\}$$
$$d\tau\,\mathrm{H}(t-bh)\,\mathrm{H}(-\cos\theta) \quad (54)$$

and

$$K_{III}^{(D)}(t) = \frac{\varepsilon_{11}k_v^2}{e_{15}(\sqrt{1-b^2v^2}-k_v^2)}K_{III}^{(\tau)}(t)\,, \quad (55)$$

where

$$\eta^+ = \left\{\left[(l+vbr)t-b^2vh^2\right]+i\,|h|\sqrt{t^2-b^2h^2-b^2\left[(l+vbr)-tv\right]^2}\right\}\Big/\left[(l+vbr)^2+(1-b^2v^2)h^2\right],$$

$$\eta_i^+ = \left\{\left[(l+vbr)\,t-b^2vh^2\right]+|h|\sqrt{b^2h^2+b^2\left[(l+vbr)-tv\right]^2-t^2}\right\}\Big/\left[(l+vbr)^2+(1-b^2v^2)h^2\right]+i\varepsilon$$

and $\theta = \cos^{-1}(l/r)$. The first term in (54) is due to the contribution of the mechanical wave, while the second term represents the electromagnetic wave. It is noted that the corresponding solutions of the stress intensity factor and the electric displacement intensity factor for the static problem are

$$K_{III}^{(\tau),s} = p\sqrt{\frac{2}{\pi r}}\sin\left(\frac{\theta}{2}\right) \quad (56)$$

and

$$K_{III}^{(D),s} = \frac{\varepsilon_{11}k_v^2}{e_{15}(1-k_v^2)}K_{III}^{(\tau),s}\,. \quad (57)$$

4. NUMERICAL RESULTS

The transient solutions of dynamic stress intensity factor and dynamic electric displacement intensity factor are obtained in simple, closed forms in the previous section. Numerical calculations will be carried out and discussed in this section. At time $t = 0$, a dynamic anti-plane concentrated loading with magnitude $2p$ is applied at $x = l$, $y = h$. It is assumed that the propagating crack is contained a permeable vacuum environment, such that the electrostatic potential is nonzero. The geometrical configuration of the problem is depicted in Fig. 2. The piezoelectric material to be considered in numerical calculations is PZT4 and the material constants of PZT4 are listed in Table 1.

Figures 3 and 4 represent the normalized dynamic stress intensity factors and dynamic electric displacement intensity factors versus normalized time for different values of crack speed v for $\theta = 30°$. In Fig. 3, there is a small illustration on the left hand side which presents the transient response of $K_{III}^{(\tau)}$ for the stationary crack ($v = 0$) approaches the correspondent static value for longer time. It is noted that the transient result for the stationary crack will jump to the static value for the pure elastic material as indicated by Ma and Chen [28]. The normalized dynamic stress intensity factor and dynamic electric displacement intensity factor of the propagating crack for $\theta = 60°$ are presented in Figs. 5 and 6. The transient response of dynamic intensity factors for the stationary crack keeps zero before the piezoelectric shear wave arrives at the crack tip and approaches the static value immediately when the piezoelectric shear wave passes through the tip at time $t/br = 1$. In general, the transient response of dynamic intensity factors for the propagating crack keeps zero before the piezoelectric shear wave arrives at the crack tip and has positive value when the piezoelectric shear wave passes through the tip at time $t/br = 1$. It keeps increasing due to the fact that the propagating crack tip close to the applied loading and then decreases smoothly after the crack propagates away from the applied loading.

Figures 7 and 8 show the normalized dynamic stress intensity factors and dynamic electric displacement intensity factors versus normalized time for different values of crack speed v for $\theta = 120°$. In Figs. 7 and 8, there are small illustrations on the left hand side which present the transient responses of $K_{III}^{(\tau)}$ and $K_{III}^{(D)}$ at time $t/br = 0.866 \sim 1$. The electromagnetic wave is the first wave arrival at the crack tip at the normalized time equal to 0.866. The transient response of dynamic intensity factors for the stationary crack increases

Table 1 The material properties of PZT4 piezoelectric material

piezo-electric material	c_{44} (N m^{-2})	e_{15} (C m^{-1})	ε_{11} (F m^{-1})	ρ (kg m^{-3})	c (m s^{-1})	k_v	c_{bg} (m s^{-1})
PZT4	2.56×10^{10}	12.70	6.46×10^{-9}	7500	2596.26	2.599×10^{-2}	2258.02

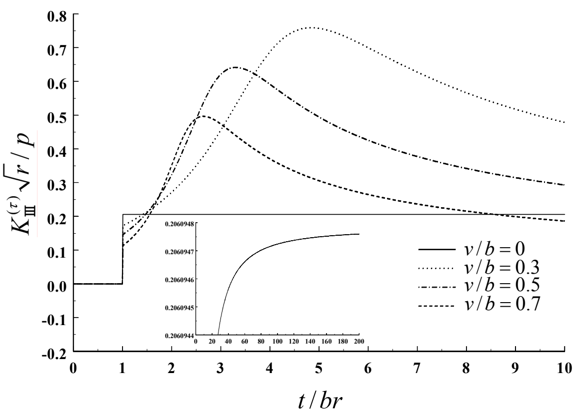

Fig. 3 Normalized dynamic stress intensity factors versus normalized time for different values of crack speed v in PZT4 for $\theta = 30°$

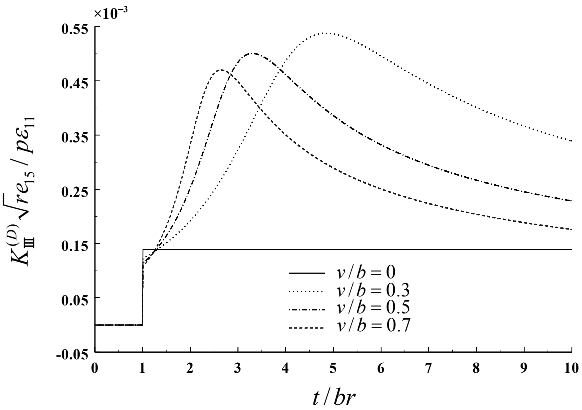

Fig. 4 Normalized dynamic electric displacement intensity factors versus normalized time for different values of crack speed v in PZT4 for $\theta = 30°$

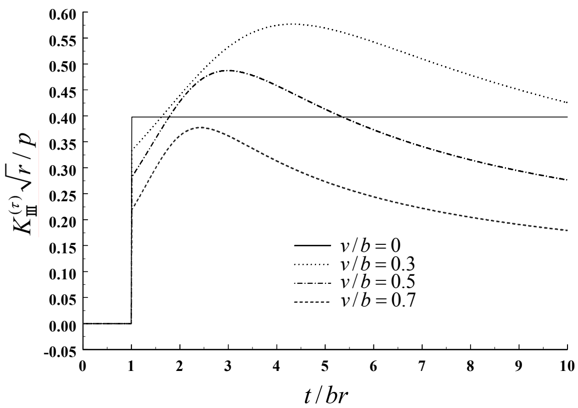

Fig. 5 Normalized dynamic stress intensity factors versus normalized time for different values of crack speed v in PZT4 for $\theta = 60°$

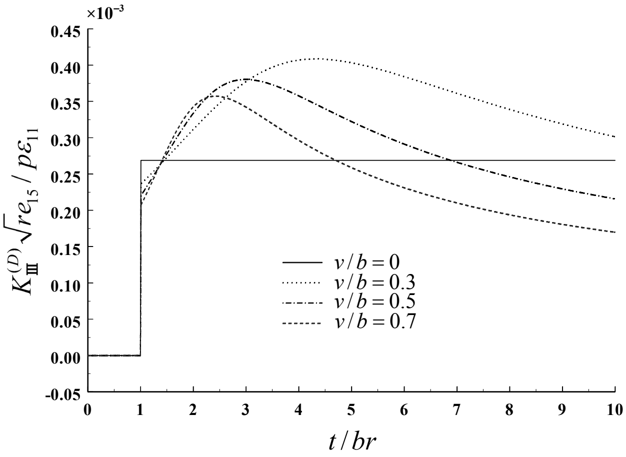

Fig. 6 Normalized dynamic electric displacement intensity factors versus normalized time for different values of crack speed v in PZT4 for $\theta = 60°$

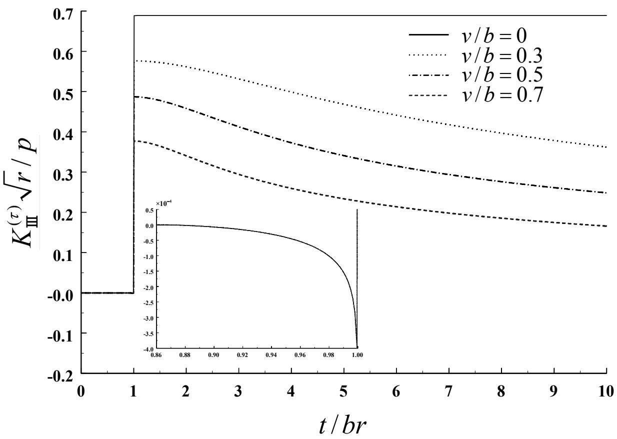

Fig. 7 Normalized dynamic stress intensity factors versus normalized time for different values of crack speed v in PZT4 for $\theta = 120°$

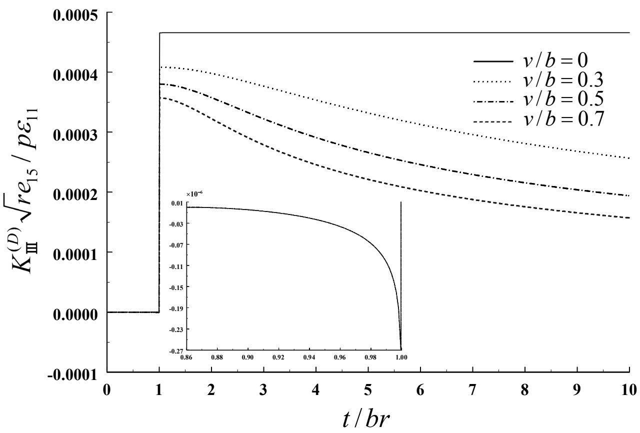

Fig. 8 Normalized dynamic electric displacement intensity factors versus normalized time for different values of crack speed v in PZT4 for $\theta = 120°$

smoothly with negative value after the electromagnetic wave arrives at the crack tip and approaches the static value immediately when the piezoelectric shear wave passes through the tip at time $t/br = 1$. For the propagating crack case, the stress intensity factor jumps to a positive value at time $t/br = 1$, and then decreases after the crack propagates with a constant velocity. The transient behavior of the dynamic electric displacement intensity factor is similar to that of the dynamic stress intensity factor. In order to present the influence of loading's position on dynamic intensity factors, the dynamic anti-plane concentrated loading is applied close to the crack faces gradually by increasing θ. Figures 9 and 10 indicate the normalized dynamic stress intensity factors and dynamic electric displacement intensity factors versus normalized time for θ = 150°. The normalized dynamic stress intensity factor and dynamic electric displacement intensity factor of the propagating crack for θ = 179° are presented in Figs. 11 and 12. It shows clearly from Figs. 7 ~ 12 that the dynamic stress intensity factor and dynamic electric displacement intensity factor for the stationary crack increase its value with increase θ. However, the contribution of dynamic intensity factor from the electromagnetic wave is relatively small. The values of dynamic intensity factors are small for high crack propagation velocity. It is worthy to note that the transient result of dynamic intensity factors will approach the correspondent static value after the incident mechanical wave has passed the crack tip.

5. CONCLUSIONS

The phenomena of crack propagation, arrest and branching are important subjects in the areas of dynamic fracture analysis, it is very important to have analytical results for these problems. In this work, the transient response of a propagating crack subjected to dynamic anti-plane body forces for the piezoelectric material is investigated. An assumption is made that the propagating crack is abutted to permeable vacuum at crack surfaces. A new fundamental solution for the piezoelectric material is proposed and the transient response of the propagating crack is determined by superposition of the fundamental solution in the Laplace transform domain. Finally, exact analytical transient solutions for the dynamic stress intensity factor and the dynamic electric displacement intensity factor are obtained by using the Cagniard method of Laplace inversion and are expressed in explicit forms. Each term in the formulations has its own physical meaning. Note that the crack propagation speed is less than the sub-Bleustein-Gulyaev speed ($v < c_{bg}$). It is found that the dynamic result of intensity factors for the stationary crack will approach the correspondent static value after the incident mechanical wave has passed the stationary crack tip. However the transient result for the stationary crack will jump to the static value for the pure

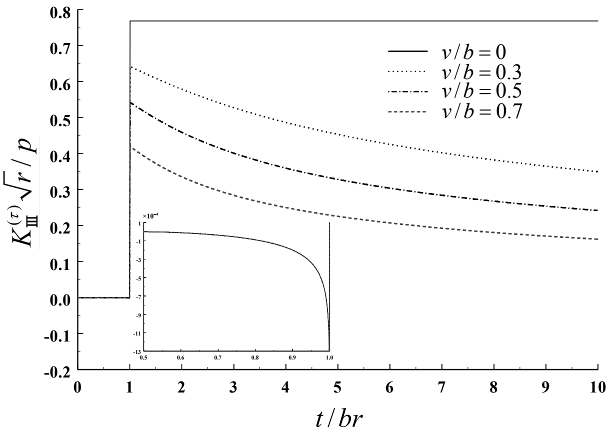

Fig. 9 Normalized dynamic stress intensity factors versus normalized time for different values of crack speed v in PZT4 for θ = 150°

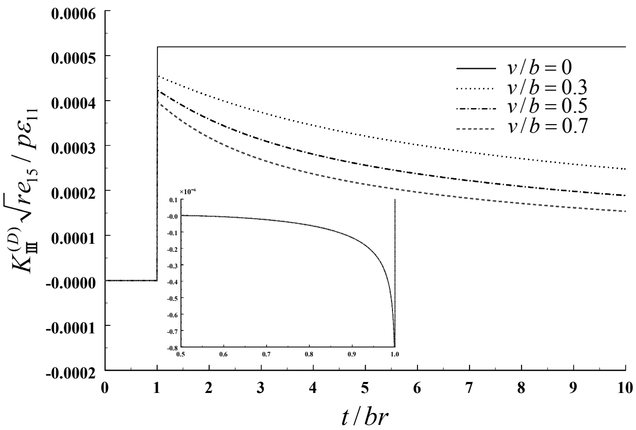

Fig. 10 Normalized dynamic electric displacement intensity factors versus normalized time for different values of crack speed v in PZT4 for θ = 150°

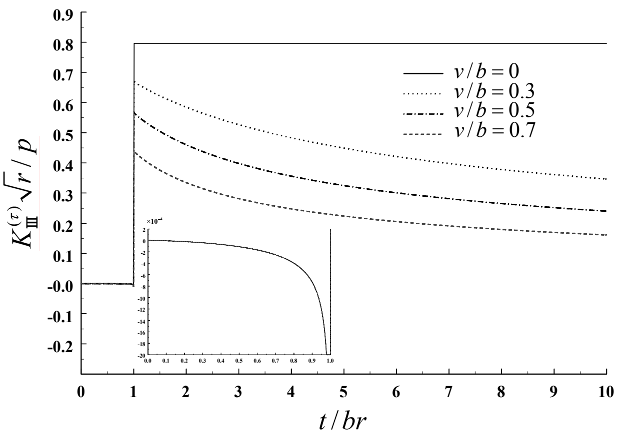

Fig. 11 Normalized dynamic stress intensity factors versus normalized time for different values of crack speed v in PZT4 for θ = 179°

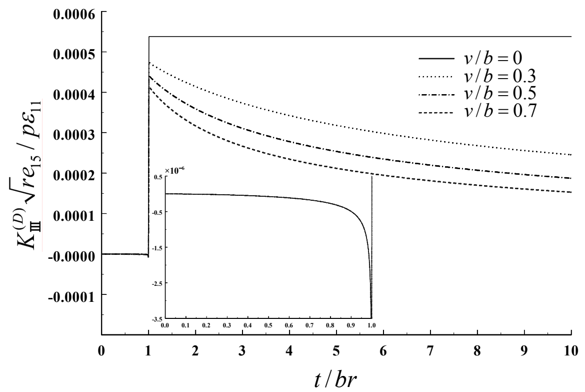

Fig. 12 Normalized dynamic electric displacement intensity factors versus normalized time for different values of crack speed v in PZT4 for $\theta = 179°$

elastic material. It should be reminded that only the intensities are derived in this study. The transient full-field solutions for the crack propagation problem can also be obtained by using the fundamental solutions presented in Section 2.

ACKNOWLEDGMENTS

The authors gratefully acknowledge the financial support of this research by the National Science Council (Republic of China) under Grant NSC 92-2212-E-002-065.

REFERENCES

1. Noble, B., *Method Based on the Wiener-Hopf Technique*, Elmsford, New York (1958).
2. Cagnard, L., *Reflexion et Refraction des Ondes Seismiques Progressives*, McGraw-Hill, New York (1939).
3. de Hoop, A. T., "A Modification of Cagniard's Method for Solving Seismic Pulse Problems," *Appl. Sci. Res. Sect. B,* 8, pp. 349–360 (1960).
4. Pohanka, R. C. and Smith, P. L., *Recent Advances in Piezoelectric Ceramics*, Marcel Dekker, New York (1988).
5. Bleustein, J. L., "A New Surface Wave in Piezoelectric Materials," *Appl. Phys. Lett.,* 13, pp. 412–413 (1968).
6. Gulyaev, Y. V., "Electro-Acoustic Surface Waves in Solids," *Sov. Phys.,* JETP 9, pp. 37–38 (1969).
7. Stoneley, R., "Elastic Waves at the Surface of Separation of Two Solids," *Proc. R. Soc.,* A106, pp. 416–428 (1924).
8. Daros, C. H., "On Modeling Bleustein-Gulyaev Waves in Non-Homogeneous, Transversely Isotropic, Piezoelectric Media via Stress Equations of Motion," *Acta. Mech.,* 163, pp. 121–126 (2003).
9. Yoffe, E. H., "The Moving Griffith Crack," *Philosophical Magazine*, 42, pp. 739–750 (1951).
10. Achenbach, J. D., "Brittle and Ductile Extension of a Finite Crack by a Horizontally Polarized Shear Wave," *Int. J. Eng. Sci.,* 8, pp. 947–966 (1970).
11. Freund, L. B., "Crack Propagation in an Elastic Solid Subjected to General Loading — I. Constant Rate of Extension," *J. Mech. Phys. Solids*., 20, pp. 129–140 (1972).
12. Ma, C. C. and Hou, Y. C., "Theoretical Analysis of the Transient Response for a Stationary In-plane Crack Subjected to Dynamic Impact Loading," *Int. J. Engng Sci*., 28, pp. 1321–1329 (1990).
13. Ma, C. C. and Hou, Y. C., "Transient Analysis for Anti-plane Crack Subjected to Dynamic Loadings," *J. Appl. Mech.*, 58, pp. 703–709 (1991).
14. Li, S. and Mataga, P. A., "Dynamic Crack Propagation in Piezoelectric Materials — Part I. Electrode Solution," *J. Mech. Phys. Solids.*, 44, pp. 1799–1830 (1996).
15. Li, S. and Mataga, P. A., "Dynamic Crack Propagation in Piezoelectric Materials — Part II. Vacuum Solution," *J. Mech. Phys. Solids.*, 44, pp. 1831–1866 (1996).
16. Ing, Y. S. and Ma, C. C., "Transient Response of a Finite Crack Subjected to Dynamic Anti-plane Loading," *Int. J. Fracture*, 82, pp. 345–362 (1996).
17. Ing, Y. S. and Ma, C. C., "Dynamic Fracture Analysis of a Finite Crack Subjected to an Incident Horizontally Polarized Shear Wave," *Int. J. Solids Struct.*, 34, pp. 895–910 (1997).
18. Chen, Z. T. and Yu, S. W., "Anti-plane Yoffe Crack Problem in Piezoelectric Materials," *Int. J. Fract.,* 84, pp. L41–L45 (1997).
19. Kwon, S. M. and Lee, K. Y, "Analysis of Stress and Electric Field in a Rectangular Piezoelectric Body with a Center Crack under Anti-plane Shear Loading," *Int. J. Solids Struct.,* 37, pp. 4859–4869 (2000).
20. To, A. C., Li, S. and Glaser, S. D., "On Scattering in Dissimilar Piezoelectric Materials by a Semi-infinite Interfacial Crack," *Q. J. Mech. Appl. Math.*, 58, pp. 309–331 (2005).
21. Freund, L. B., "The Stress Intensity Factor due to Normal Impact Loading of the Faces of a Crack," *Int. J. Eng. Sci.*, 12, pp. 179–189 (1974).
22. Ing, Y. S. and Wang, M. J., "Explicit Transient Solutions for a Mode III Crack Subjected to Dynamic Concentrated Loading in a Piezoelectric Material," *Int. J. Solids Struct.*, 41, pp. 3849–3864 (2004).
23. Tsai, C. H. and Ma, C. C., "Transient Analysis of a Semi-infinite Crack Subjected to Dynamic Concentrated Force," *J. Appl. Mech.*, 59, pp. 804–811 (1992).
24. Ma, C. C. and Chen, S. K., "Exact Transient Full-field Analysis of an Anti-plane Subsurface Crack Subjected to Dynamic Impact Loading," *J. Appl. Mech.,* 61, pp. 649–655 (1994).
25. Tsai, C. H. and Ma, C. C., "Transient Analysis of a Propagating In-plane Crack in a Finite Geometry Body Subjected to Static Loadings," *J. Appl. Mech.*, 64, pp. 620–628 (1997).
26. Tsai, C. H. and Ma, C. C., "Theoretical Transient Analysis of the Interaction Between a Dynamically Propagating In-plane Crack and Traction Free Boundaries," *J. Appl. Mech.*, 64, pp. 819–827 (1997).

27. Yang, X. H., Dong, L., Chen, C. Y., Wang, C. and Hu, Y. T., "Damage Extension Forces and Piezoelectric Fracture Criteria," *Journal of Mechanics*, 20, pp. 277–283 (2004).
28. Ma, C. C. and Chen, S. K., "Exact Transient Analysis of an Anti-plane Semi-infinite Crack Subjected to Dynamic Body Forces," *Wave Motion*, 17, pp. 161–171 (1993).

(Manuscript received July 3, 2006,
accepted for publication October 2, 2006.)